Available online at www.sciencedirect.com
ScienceDirect
Journal of the European Ceramic Society 29 (2009) 3379–3385
www.elsevier.com/locate/jeurceramsoc

Effect of Ti_5Si_3 on wear properties of $Ti_3Si(Al)C_2$

Yonglai Liu [a,b], Jixin Chen [a], Yanchun Zhou [a,*]

[a] *Shenyang National Laboratory for Materials Science, Institute of Metal Research, Chinese Academy of Sciences, 72 Wenhua Road, Shenyang 110016, China*
[b] *Graduate School of Chinese Academy of Sciences, Beijing 100039, China*

Received 17 February 2009; received in revised form 14 June 2009; accepted 14 July 2009
Available online 5 August 2009

Abstract

Near-fully dense $Ti_3Si(Al)C_2/Ti_5Si_3$ composites were synthesized by in situ hot pressing/solid–liquid reaction process under a pressure of 30 MPa in a flowing Ar atmosphere at 1580 °C for 60 min. Compared to monolithic $Ti_3Si(Al)C_2$, $Ti_3Si(Al)C_2/Ti_5Si_3$ composites exhibit higher hardness and improved wear resistance, but a slight loss in flexural strength (about 26% lower than $Ti_3Si(Al)C_2$ matrix). In addition, $Ti_3Si(Al)C_2/Ti_5Si_3$ composites maintain a high fracture toughness (K_{IC} = 5.69–6.79 MPa $m^{1/2}$). The $Ti_3Si(Al)C_2$/30 vol.%Ti_5Si_3 composite shows the highest Vickers hardness (68% higher than that of $Ti_3Si(Al)C_2$) and best wear resistance (the wear resistance increases by 2 orders of magnitude). The improved properties are mainly ascribed to the contribution of hard Ti_5Si_3 particles, and the strength degradation is mainly due to the lower Young's modulus and strength of Ti_5Si_3.

Keywords: $Ti_3Si(Al)C_2$; Ti_5Si_3; Composites; In situ hot pressing; Wear resistance

1. Introduction

As a member of layered ternary ceramics, Ti_3SiC_2 possesses a unique combination of the properties of both metals and ceramics, such as low density, high strength and modulus, good thermal and electrical conductivity, damage tolerance at room temperature, and excellent resistance to thermal shock and oxidation below 1100 °C, and above all, good machinability.[1–8] However, the application of Ti_3SiC_2 was limited because of its low hardness (Vickers hardness of 4 GPa) and poor wear resistance.

The essential reason of the low hardness and poor wear resistance of Ti_3SiC_2 was the weak bonding between the Ti–C–Ti–C–Ti covalent bond chain and Si atomic layer, which was indicated by previous experimental and theoretical studies.[9–12] Many works have been carried out to study the friction and wear behaviors of Ti_3SiC_2 and improve hardness and wear resistance of Ti_3SiC_2. Generally, incorporating hard particles such as SiC[13] and Al_2O_3[14], or surface strengthening[15,16] have been reported to improve hardness and wear resistance of Ti_3SiC_2.

In this work, titanium silicide, Ti_5Si_3, was used as reinforcing particles to enhance the hardness and wear resistance of Ti_3SiC_2 for several reasons. Firstly, Ti_5Si_3 has low density (ρ = 4.32 g/cm^3), high melting point (2130 °C),[17] high hardness (Vickers hardness of 9.7 GPa), good high-temperature strength.[18,19] In addition, Ti_5Si_3 exhibits similar thermal expansion coefficient to that of Ti_3SiC_2.[17–26] Hence, Ti_5Si_3 was chosen to prepare Ti_3SiC_2/Ti_5Si_3 composites in order to enhance the hardness and wear resistance of Ti_3SiC_2.

The composites were prepared by the in situ hot pressing/solid–liquid reaction process which was used to prepare Ti_3SiC_2 in our previous work.[27] The hardness, flexural strength, fracture toughness and tribological properties of the composites were investigated.

2. Experimental

2.1. Material preparation

Ti_3SiC_2 and Ti_5Si_3 were synthesized from elemental powders by Zhou et al.[27], Sato et al.[28] and Rosenkranz et al.[21]. So Ti_3SiC_2/Ti_5Si_3 composites were possibly to be prepared from

* Corresponding author at: High-performance Ceramic Division, Shenyang National Laboratory for Materials Science, Institute of Metal Research, Chinese Academy of Sciences, 72 Wenhua Road, Shenyang 110016, China.
Tel.: +86 24 23971765; fax: +86 24 23891320.
E-mail address: yczhou@imr.ac.cn (Y. Zhou).

0955-2219/$ – see front matter © 2009 Elsevier Ltd. All rights reserved.
doi:10.1016/j.jeurceramsoc.2009.07.012

elemental powders, and this possibility was proved by our experiment. In this work, bulk $Ti_3Si(Al)C_2$ and $Ti_3Si(Al)C_2/Ti_5Si_3$ composites were prepared by the in situ hot pressing/solid–liquid reaction process.[27] Commercially available elemental powders of Ti (99%, −300 mesh), Si (99%, −400 mesh), Al (99.5%, −200 mesh) and graphite (98%, −200 mesh) were used as initial materials. Al was added to eliminate TiC by forming a $Ti_3Si(Al)C_2$ solid solution. The contents of Ti_5Si_3 were adjusted by controlling the ratio of Ti and Si in the initial materials.

First, elemental powders of Ti, Si, Al and graphite were weighed according to the target compositions, and then dry mixed in a polyurethane jar for 15 h. After mixing, the powder mixtures were put into an Ø50 mm BN-coated graphite mold, and cold pressed at 10 MPa. Afterward, the compact mixture was hot pressed at 1580 °C under 30 MPa for 60 min in a flowing Ar atmosphere.

The as-prepared plate was about $Ø50 \times 10\,mm^3$ in size. Before investigating the mechanical properties and wear resistance, a surface layer of 0.8 mm thick was removed to eliminate the contamination.

2.2. Characterization of $Ti_3Si(Al)C_2/Ti_5Si_3$ composites

The densities of the $Ti_3Si(Al)C_2/Ti_5Si_3$ composites with different Ti_5Si_3 contents were measured by Archimedes method. And the phase compositions were identified by X-ray diffraction (XRD) using powders drilled from the bulk samples. The XRD data were collected by a step-scanning diffractometer with CuKα radiation (Rigaku D/max-2400, Tokyo, Japan). In order to determine the contents of Ti_5Si_3 in $Ti_3Si(Al)C_2/Ti_5Si_3$ composites, Rietveld refinement was conducted using Rietan-2000 program[29] for quantitative phase analysis.

The Vickers hardness was measured by a digital microhardness tester at a load of 10 N with a dwell time of 15 s. The dynamic elastic modulus of $Ti_3Si(Al)C_2/Ti_5Si_3$ composites was determined by an impulse excitation apparatus (IEA) (IMCE, Diepenbeek, Belgium) using specimens of 3 mm × 15 mm × 40 mm in size. The room temperature flexural strength and fracture toughness were determined on a universal-testing machine. Three-point bending tests were performed to measure the flexural strength and fracture toughness (K_{IC}). The sample size for flexural strength testing was 3 mm × 4 mm × 36 mm and the crosshead speed was 0.5 mm/min. Fracture toughness was determined using the single-edge notched beam method with specimen dimensions of 4 mm × 8 mm × 36 mm. A notch of 4 mm in length and 0.15 mm in width was made by the electrical discharge method (EDM). The crosshead speed for fracture toughness testing was 0.05 mm/min.

To reveal the grain size of $Ti_3Si(Al)C_2$ and Ti_5Si_3, samples were mechanically polished and then etched by an HNO_3:HF:H_2O (1:1:2) solution before SEM observation. The microstructure of $Ti_3Si(Al)C_2/Ti_5Si_3$ composites was observed by a SUPRA 35 scanning electron microscope (SEM) (LEO, Oberkochen, Germany) equipped with an energy-dispersive spectroscopy (EDS) system.

The sliding friction and wear tests were carried out on a commercially available micro-tribometer (UMT-2, CETR, California, USA). A reciprocating ball on flat configuration was applied, where an automatic device moved the flat specimen back and forth under a fixed ball. The normal load was applied downward through the upper steel ball (Ø4 mm, AISI-52100 bearing steel, 7.85 g cm^{-3}, HRc 62-63) to the flat. Flats of 3 mm × 4 mm × 16 mm were cut from the as-prepared $Ti_3Si(Al)C_2/Ti_5Si_3$ composites by electrical discharge method (EDM). The test surface of samples was ground and polished with 0.5 μm diamond paste. Before friction and wear tests, all specimens were cleaned in an ultrasonic bath with acetone and ethanol, dried at 120 °C for 2 h and then cooled down to room temperature. Each specimen was weighed using an electronic balance with an accuracy of 10^{-5} g before wear test. After testing the samples were cleaned in an ultrasonic bath with acetone and then weighed again.

During the wear tests the upper ball was immobile and only allowed a vertical movement to adjust the relative position. The friction force, induced between the steel ball and the sample, was measured by a force sensor and recorded in a computer automatically. A linear reciprocating ball sliding on an athletic flat specimen (3 mm × 4 mm × 16 mm) was adopted at room temperature with a relative humidity of 35 ± 5%. The ball rubbed the surfaces (4 mm × 16 mm) of Ti_3SiC_2 and $Ti_3Si(Al)C_2/Ti_5Si_3$ composites with the point contact wear mode under non-lubrication condition. The tests were conducted under loads of 5, 10 and 20 N with a stroke length 8.5 mm at a sliding speed 56 mm s^{-1} for 1000 s, the total sliding distance of the test was 56 m. Friction coefficient was measured by an analog-to-digital converter and recorded in a computer. The wear rates of the composites and wear loss of AISI-52100 bearing steel ball were calculated by

$$W = \frac{V}{PL} = \frac{\chi}{\rho PL} \quad (1)$$

$$\chi = m_1 - m_0 \quad (2)$$

where V is the wear volumes of the composites obtained by measuring the weight loss in a microbalance (accuracy, 10^{-5} g) and from the density (ρ) after ultrasonic cleaning, P is the force and L is the sliding distance. m_1 and m_0 are the mass of AISI-52100 bearing steel ball before and after test, respectively. For each experimental condition and material, three tests were performed. The worn surface of samples and counterpair bearing steel were investigated by SEM. The wear debris collected on the worn track of materials was analyzed by XRD, SEM and EDS.

3. Results and discussion

3.1. Synthesis, phase composition, and microstructure

$Ti_3Si(Al)C_2/Ti_5Si_3$ composites were synthesized at 1580 °C with extra Ti and Si powder to control the content of Ti_5Si_3. The impurity phase such as TiC can be eliminated by partial substitution of Si with Al.[30,31] Based on these facts, 10 at.% of

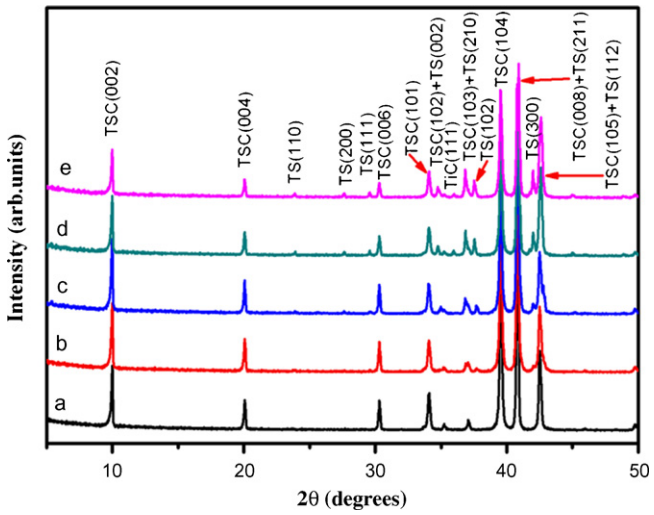

Fig. 1. X-ray diffraction patterns of the materials synthesized by in situ hot pressing/solid–liquid reaction process: (a) TSC; (b) TSC/5TS; (c) TSC/10TS; (d) TSC/20TS; (e) TSC/30TS.

Al was added into the initial materials to make sure that no TiC existed in the final composites. Therefore, the true composition of the matrix is $Ti_3Si_{0.9}Al_{0.1}C_2$ and is denoted as $Ti_3Si(Al)C_2$ thereafter for short.

Fig. 1 shows the XRD patterns of $Ti_3Si(Al)C_2$ and $Ti_3Si(Al)C_2/Ti_5Si_3$ composites with different amounts of Ti_5Si_3. The crystalline phases are identified as $Ti_3Si(Al)C_2$ and Ti_5Si_3. No peaks from impurity phases such as TiC and SiC can be detected via XRD in $Ti_3Si(Al)C_2$, $Ti_3Si(Al)C_2$/5 vol.%Ti_5Si_3 and $Ti_3Si(Al)C_2$/10 vol.%Ti_5Si_3 composites. However, a small amount of TiC impurity appears in $Ti_3Si(Al)C_2$/20 vol.%Ti_5Si_3 and $Ti_3Si(Al)C_2$/30 vol.%Ti_5Si_3 composites because of the large amounts of Ti and Si in the initial materials. The content of Ti_5Si_3 in the $Ti_3Si(Al)C_2/Ti_5Si_3$ composites is listed in Table 1, which is determined by Rietveld quantitative phase analysis. It can be seen that the calculated Ti_5Si_3 content is closed to the target value in the $Ti_3Si(Al)C_2/Ti_5Si_3$ composites. The reliability indices of *R*-p and *R*-wp are less than 15 and 20, respectively, which denote that the calculated results are reliable. For the sake of brevity, $Ti_3Si(Al)C_2$ and $Ti_3Si(Al)C_2/Ti_5Si_3$ composites with 5, 10, 20 and 30 vol.% Ti_5Si_3 are named as TSC, TSC/5TS, TSC/10TS, TSC/20TS and TSC/30TS, respectively.

Table 1
The target Ti_5Si_3 volume contents in $Ti_3Si(Al)C_2/Ti_5Si_3$ composites compared with those calculated by Rietveld method.

Samples	Ti_5Si_3 (vol.%) (target)	Ti_5Si_3 (vol.%) (calculated)	*R*-wp	*R*-p
TSC	0	0	15.71	9.75
TSC/5TS	5	4.23	15.35	9.96
TSC/10TS	10	10.61	15.93	10.81
TSC/20TS	20	23.20	17.68	12.31
TSC/30TS	30	30.64	18.35	12.98

The measured densities of the composites decline with the increment of Ti_5Si_3 content, which is attributed to the lower density of Ti_5Si_3 than that of $Ti_3Si(Al)C_2$. All samples prepared by this process are near fully dense (≥98% of the theoretical density). Fig. 2 displays the backscattered electron images of the polished surfaces of TSC, TSC/10TS, TSC/20TS and TSC/30TS composites. In Fig. 2(b–d), the light grains are rich in Ti, Si and less in C by EDS and are corresponding to Ti_5Si_3. The gray grains are composed of Ti, Si, Al and C, which are recognized as $Ti_3Si(Al)C_2$. The Ti_5Si_3 platelets are uniformly dispersed in the $Ti_3Si(Al)C_2$ matrix. The average grain sizes

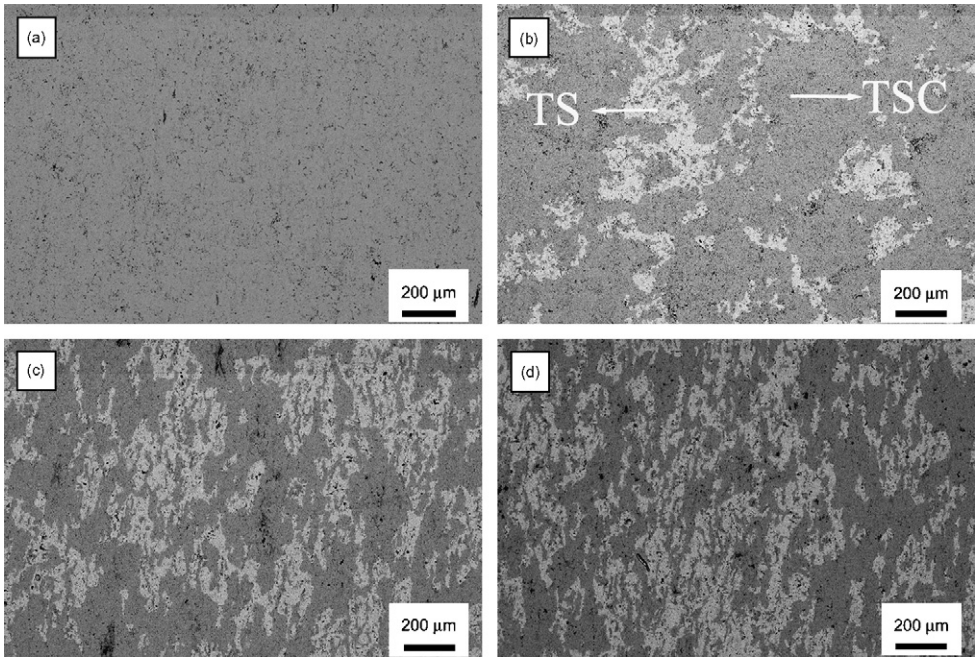

Fig. 2. Backscattered electron images of the polished surfaces of (a) TSC; (b) TSC/10TS; (c) TSC/20TS; (d) TSC/30TS. The dark gray phase is $Ti_3Si(Al)C_2$ and the light phase is Ti_5Si_3.

Table 2
Measured average grain sizes of $Ti_3Si(Al)C_2$ and Ti_5Si_3 grains in the $Ti_3Si(Al)C_2/Ti_5Si_3$ composites.

Samples	Average grain size			
	$Ti_3Si(Al)C_2$		Ti_5Si_3	
	Grain length (μm)	Grain width (μm)	Grain length (μm)	Grain width (μm)
TSC	17.2	9.7		
TSC/10TS	14.5	6.1	13.9	4.4
TSC/20TS	14.3	4.9	10.5	3.9
TSC/30TS	13.7	4.8	10.7	4.3

of $Ti_3Si(Al)C_2$ gradually reduce with increasing Ti_5Si_3 content (not shown). Table 2 compared the measured average grain size of $Ti_3Si(Al)C_2$ and Ti_5Si_3 in the composites.

3.2. Mechanical properties

Before investigating the tribological behavior, the mechanical properties of $Ti_3Si(Al)C_2/Ti_5Si_3$ composites are tested. Fig. 3 shows the Vickers hardness of $Ti_3Si(Al)C_2$ matrix and $Ti_3Si(Al)C_2/Ti_5Si_3$ composites versus Ti_5Si_3 content. It can be seen that the measured Vickers hardness increases almost linearly from 3.6 ± 0.6 GPa for monolithic TSC to 6.3 ± 0.9 GPa for the TSC/30TS with the increment of Ti_5Si_3 content. Like Ti_3SiC_2,[4] no indentation-induced cracks are observed at the corner of the indentation of the composites, which indicates that the $Ti_3Si(Al)C_2/Ti_5Si_3$ composites are tolerant to the surface damage even when the Ti_5Si_3 volume content reaches 30%. SEM observation on the morphology of the indents reveals that the grains in the composites are squeezed out from the indentation and piled up at the perimeter of the indent. Many grains are broken into debris or delaminated under shear stress. The microstructure of the composites in regions far from the indent remains unchanged, namely, the damage is confined to the surface indent.

The flexural strength and fracture toughness of $Ti_3Si(Al)C_2/Ti_5Si_3$ composites versus Ti_5Si_3 content are shown in Fig. 4. The flexural strength decreases from initial 382 MPa for $Ti_3Si(Al)C_2$ matrix to minimum 267 MPa for TSC/10TS, because Ti_5Si_3 has a lower Young's modulus and strength than $Ti_3Si(Al)C_2$ matrix and has no ability to strengthen $Ti_3Si(Al)C_2$. But the flexural strength maintains at a stable value of about 270 MPa with further increase of Ti_5Si_3 content from 10 to 30 vol.%. One possible reason of this stable value of flexural strength is grain refinement with the increment of Ti_5Si_3 content. The fracture toughness declines slightly from initial 6.39 MPa $m^{1/2}$ for TSC to minimum 5.69 MPa $m^{1/2}$ for TSC/10TS, and then keeps at a stable value of 6.80 MPa $m^{1/2}$ for TSC/20TS and TSC/30TS.

3.3. Wear behavior

The ratio of hardness to Young's modulus, H/E, has been proposed as one of the key parameters controlling wear.[32] A higher value of H/E means that the materials have improved resistance to scratching in the contact area during dry sliding.[33,34]

The results in the previous section show that hardness increases with the increment of Ti_5Si_3 content, and the Young's modulus of Ti_5Si_3 ($E = 156$ GPa) is lower than that of $Ti_3Si(Al)C_2$, so wear resistance can be improved.

During a continuous reciprocating test with a total sliding distance of 56 m at a velocity of 0.056 m s^{-1} and under a constant loads of 20 N, the typical friction coefficients of $Ti_3Si(Al)C_2$ and $Ti_3Si(Al)C_2/Ti_5Si_3$ composite against AISI-52100 bearing steel balls (HR_C 62-63) were compared in Fig. 5. It is found that the

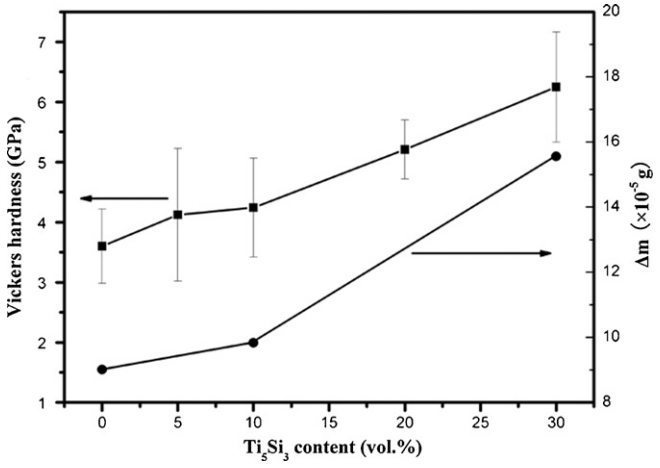

Fig. 3. The Vickers hardness of $Ti_3Si(Al)C_2/Ti_5Si_3$ composites and weight loss of the corresponding ball AISI-52100 bearing steel ball in non-lubrication reciprocation motion tests vs. Ti_5Si_3 content.

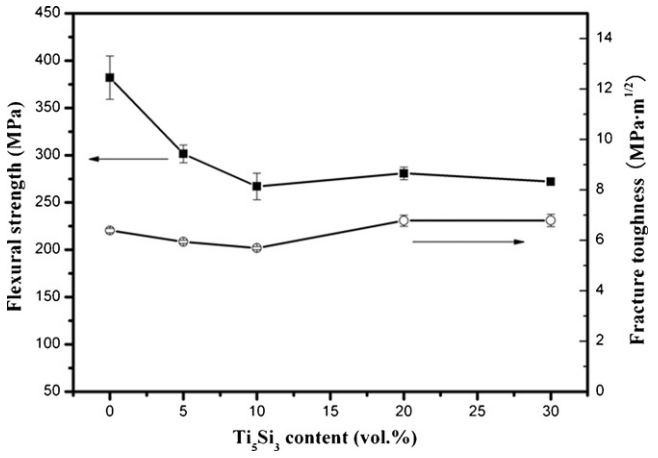

Fig. 4. Flexural strength and fracture toughness (K_{IC}) vs. Ti_5Si_3 content in $Ti_3Si(Al)C_2/Ti_5Si_3$ composites.

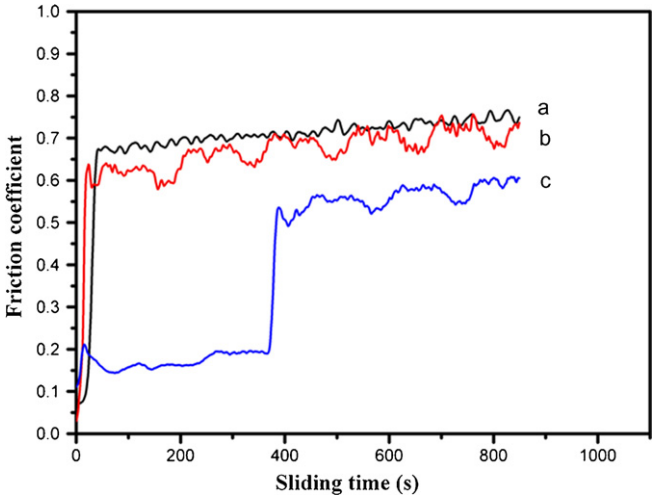

Fig. 5. Friction coefficient vs. sliding time for (a) TSC; (b) TSC/10TS; (c) TSC/30TS at 20 N against AISI-52100 bearing steel ball in non-lubrication reciprocation motion tests.

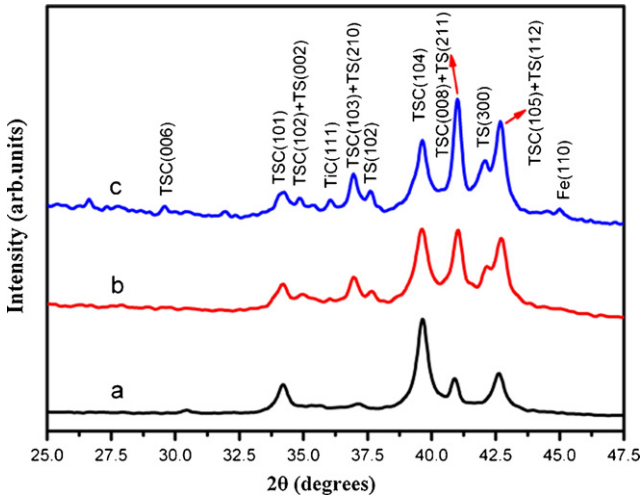

Fig. 7. X-ray diffraction patterns of the collected debris from the worn tracks of (a) TSC, (b) TSC/10TS and (c) TSC/30TS against AISI-52100 bearing steel ball in non-lubrication reciprocation motion test under a load of 20 N.

friction coefficient of monolithic $Ti_3Si(Al)C_2$ at the beginning is usually as low as 0.07–0.08 and then reaches a stable value of 0.70–0.80 after 35 s of sliding under 20 N. In contrast, the friction coefficient of TSC/10TS composite increases up to 0.60–0.65 after 20 s, however, two friction regimes for TSC/30TS were observed[11], i.e., the friction coefficient of TSC/30TS was as low as 0.07–0.08 for about 400 s and then maintains at a stable value of 0.50–0.55. Hence, the TSC/30TS composite represents a lower steady friction coefficient than that of monolithic $Ti_3Si(Al)C_2$. Fig. 6 displays the variation in steady friction coefficients after 800 s as a function of the applied load. The friction coefficient of monolithic $Ti_3Si(Al)C_2$ maintains at 0.25–0.30 as the load changing from 5 to 10 N and then increases to 0.70–0.80 at 20 N. Compared to $Ti_3Si(Al)C_2$, the friction coefficients of the $Ti_3Si(Al)C_2/Ti_5Si_3$ composites are much lower and are relatively insensitive to the applied load.

The effect of normal load on the wear rate of $Ti_3Si(Al)C_2$ (a), TSC/10TS (b), and TSC/30TS (c) against AISI-52100 bearing steel ball in non-lubrication reciprocation motion tests is shown in Fig. 6. The wear rates of $Ti_3Si(Al)C_2/Ti_5Si_3$ composites exhibit a smaller increment with increasing loads than that of $Ti_3Si(Al)C_2$. Under the load of 20 N, the wear rates of $Ti_3Si(Al)C_2$ and the composites containing 10 and 30 vol.% Ti_5Si_3 are 2.78×10^{-6}, 1.31×10^{-6}, and 2.56×10^{-7} $cm^3/N\,m$, respectively. The results indicate that the wear rate is greatly decreased with increasing Ti_5Si_3 volume content, namely, the wear resistance of $Ti_3Si(Al)C_2$ is greatly enhanced with the incorporation of the Ti_5Si_3 particles into the $Ti_3Si(Al)C_2$ matrix. With the increment of Ti_5Si_3 content, the direct load of the counterpart on the soft $Ti_3Si(Al)C_2$ matrix is effectively reduced. Thus, the deformation under the sliding ball is more likely to be elastic and the composites are expected to have smaller accumulative strain and strain energy on the contact surface, so that the wear rates are reduced.[14]

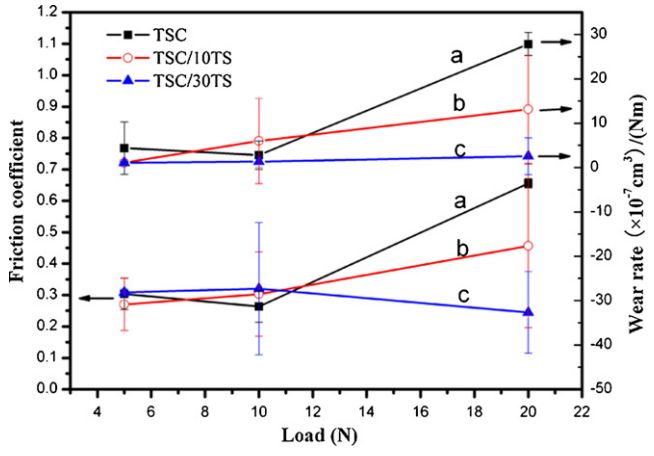

Fig. 6. Effect of normal load on the friction coefficient and wear rates of (a) TSC; (b) TSC/10TS; (c) TSC/30TS against AISI-52100 bearing steel ball in non-lubrication reciprocation motion tests.

The change of the wear loss of AISI-52100 bearing steel ball with the increase of Ti_5Si_3 content are displayed in Fig. 3. Wear loss of AISI-52100 bearing steel ball increases almost linearly with the increment of Ti_5Si_3 content. The values of wear loss are 9.0×10^{-5}, 9.8×10^{-5} and 1.6×10^{-4} g, when the volume fractions of Ti_5Si_3 are 0, 10 and 30 vol.%, respectively.

To further investigate the interactions between $Ti_3Si(Al)C_2$-based materials and the counterpart steel balls under non-lubricated conditions and to understand the effect of Ti_5Si_3 on sliding wear, the worn surfaces of the specimens, the balls as well as the wear debris were examined by SEM and XRD after tests. Typical XRD patterns of the collected wear debris from TSC, TSC/10TS and TSC/30TS composites against AISI-52100 steel balls under dry sliding tests are shown in Fig. 7. It can be found that Fe exists in the wear debris for TSC/30TS but not exists for TSC and TSC/10TS. This is a clear evidence that the fragments of iron removed from the steel balls, which indicates that the wear resistance of $Ti_3Si(Al)C_2/Ti_5Si_3$ composites increases with the increment of Ti_5Si_3 content.

Fig. 8 shows the typical worn surfaces of $Ti_3Si(Al)C_2$ and $Ti_3Si(Al)C_2/Ti_5Si_3$ composites under a load of 20 N. For TSC,

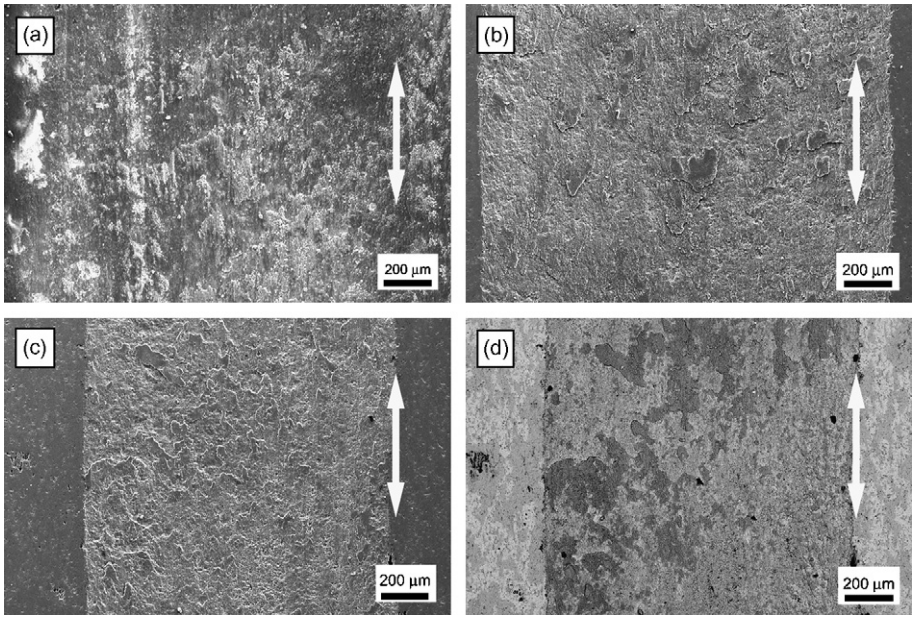

Fig. 8. SEM micrographs of the worn surfaces of $Ti_3Si(Al)C_2$ and $Ti_3Si(Al)C_2/Ti_5Si_3$ composites tested under a load of 20 N: (a) TSC (second electron image), (b) TSC/10TS (second electron image), (c) TSC/30TS (second electron image) and (d) TSC/30TS (backscattered electron image). The bright phase in (d) is Ti_5Si_3 and the dark region is the matrix. The arrows in the figures denote the sliding directions.

the worn track is irregular and uneven, and a serious plastic deformation can be seen (Fig. 8(a)). For TSC/10TS composite, $Ti_3Si(Al)C_2$ and Ti_5Si_3 particles are removed by serious abrasion, but the discontinuous extruded flats are formed on the surface (Fig. 8(b)). For TSC/30TS composite, the worn track is smooth and nearly continuous extruded flats distribute on the worn surface (Fig. 8(c)). El-Raghy et al.[12] confirmed that the average wear rates of the coarse-grained Ti_3SiC_2 were much lower because of more energy dissipation mechanisms than fine-grained Ti_3SiC_2. However, the dispersive Ti_5Si_3 particles in the $Ti_3Si(Al)C_2$ matrix effectively inhibit the deformation and fracture of the surrounding soft $Ti_3Si(Al)C_2$ matrix so that some extruded flats are formed to bear the load and weaken the scratch effect against the bearing ball.[11] Hence, it is concluded that Ti_5Si_3 particles with higher hardness can reduce the wear rates and increase the wear resistances of $Ti_3Si(Al)C_2/Ti_5Si_3$ composites due to enduring the scraping effect of the bearing ball and reducing the direct load on the soft $Ti_3Si(Al)C_2$ matrix.

Tribochemical reactions occur during the friction and wear test. According to EDS analysis, the flat areas on the worn surface are the mixtures of $Ti_3Si(Al)C_2$ particles and a large amount of silicon oxide and titanium oxide. TiO_2, SiO_2 and Fe_2O_3 probably exist in the debris collected from the wear tracks. [14,35–37] These oxides can lubricate the worn surface to weaken the scratching effect and reduce the wear rates of materials.[38–42] In this work, a large amount of silicon oxide and titanium oxide formed during non-lubrication reciprocation motion tests, which decreases the friction coefficient and wear rates by lubricating the wear surface. In addition, discontinuous extruded flats (containing SiO_2 and TiO_2) possess higher Vickers hardness than $Ti_3Si(Al)C_2$, this may be another reason of improved wear resistance.

4. Conclusions

$Ti_3Si(Al)C_2/Ti_5Si_3$ composites with near-fully density have been successfully synthesized by means of the in situ hot pressing/solid–liquid reaction process at 1580 °C for 60 min with Ti, Si, Al and graphite powders as initial materials. In the $Ti_3Si(Al)C_2/Ti_5Si_3$ composites, the Ti_5Si_3 platelets are uniformly dispersed in the $Ti_3Si(Al)C_2$ matrix. The average grain size of $Ti_3Si(Al)C_2$ gradually decreases with the increase of Ti_5Si_3 contents. The measured Vickers hardness increases almost linearly with the increment of Ti_5Si_3 content. The flexural strength drops slightly by 26% and then maintains at a stable value of about 270 MPa with the increment of Ti_5Si_3 contents. The fracture toughness declines slightly and then keeps at a stable value.

The introduction of Ti_5Si_3 has beneficial effect on the wear resistance of $Ti_3Si(Al)C_2$. Compared to $Ti_3Si(Al)C_2$, the friction coefficients and wear rates of $Ti_3Si(Al)C_2/Ti_5Si_3$ composites significantly decline (the wear resistance increases by 2 orders of magnitude). The improvement in the properties is mainly ascribed to the contribution of homogeneously dispersion of high Vickers hardness and relatively low Young's modulus Ti_5Si_3 particles in $Ti_3Si(Al)C_2/Ti_5Si_3$ composites.

Acknowledgments

This work was supported by the National Outstanding Young Scientist Foundation (No. 59925208 for Y.C. Zhou), Nature Science Foundation of China under Grant No. 50232040, No. 50302011, No. 90403027 and No. 50832008, Chinese Academy of Science and French Atomic Energy Commission.

References

1. Zhou, Y. C. and Sun, Z. M., Microstructure and mechanism of damage tolerance for Ti_3SiC_2 bulk ceramics. *Mater. Res. Innovat.*, 1999, **2**, 360–363.
2. Low, I. M., Lee, S. K. and Lawn, B. R., Contact damage accumulation in Ti_3SiC_2. *J. Am. Ceram. Soc.*, 1998, **81**(1), 225–228.
3. El-Raghy, T., Zavaliangos, A., Barsoum, M. W. and Kalidindi, S. R., Damage mechanisms around hardness indentations in Ti_3SiC_2. *J. Am. Ceram. Soc.*, 1997, **80**(3), 513–516.
4. Barsoum, M. W. and El-Raghy, T., Synthesis and characterization of a remarkable ceramic: Ti_3SiC_2. *J. Am. Ceram. Soc.*, 1996, **79**(7), 1953–1956.
5. Sun, Z. M. and Zhou, Y. C., Ab-initio calculation of titanium silicon carbide. *Phys. Rev. B*, 1999, **60**(3), 1441–1443.
6. Sun, Z. M., Zhou, Y. C. and Li, M. S., Oxidation behaviour of Ti_3SiC_2-based ceramic at 900–1300 degrees in air. *Corros. Sci.*, 2001, **43**(6), 1095–1109.
7. Barsoum, M. W. and El-Raghy, T., Oxidation of Ti_3SiC_2 in air. *J. Electrochem. Soc.*, 1997, **144**(7), 2508–2516.
8. Zhou, Y. C., Sun, Z. M., Sun, J. H., Zhang, Y. and Zhou, J., Titanium silicon carbide: a ceramic or a metal? *Z. Metall.*, 2000, **91**(4), 329–334.
9. Zhou, Y. C. and Sun, Z. M., Electronic structure and bonding properties in layered ternary carbide Ti_3SiC_2. *J. Phys.: Condens. Matter*, 2000, **12**(28), L457–L462.
10. Emmerlich, J., Gassner, G., Eklund, P., Högberg, H. and Hultman, L., Micro and macroscale tribological behavior of epitaxial Ti_3SiC_2 thin films. *Wear*, 2008, **264**, 914–919.
11. Souchet, A., Fontaine, J., Belin, M., Le Mogne, T., Loubet, J.-L. and Barsoum, M. W., Tribological duality of Ti_3SiC_2. *Tribol. Lett.*, 2005, **18**, 341–352.
12. El-Raghy, T., Blau, P. and Barsoum, M. W., Effect of grain size on friction and wear behavior of Ti_3SiC_2. *Wear*, 2000, **238**, 125–130.
13. Wan, D. T., Hu, C. F., Bao, Y. W. and Zhou, Y. C., Effect of SiC particles on the friction and wear behavior of $Ti_3Si(Al)C_2$-based composites. *Wear*, 2007, **262**, 826–832.
14. Hu, C. F., Zhou, Y. C., Bao, Y. W. and Wan, D. T., Tribological properties of polycrystalline Ti_3SiC_2 and Al_2O_3-reinforced Ti_3SiC_2 composites. *J. Am. Ceram. Soc.*, 2006, **89**(11), 3456–3461.
15. Li, C., Li, M. S. and Zhou, Y. C., Improving the surface hardness and wear resistance of Ti_3SiC_2 by boronizing treatment. *Surf. Coat. Technol.*, 2007, **201**, 6005–6011.
16. Guo, H. P., Zhang, J., Li, F. Z., Liu, Y., Yin, J. J. and Zhou, Y. C., Surface strengthening of Ti_3SiC_2 through magnetron sputtering Cu and subsequent annealing. *J. Eur. Ceram. Soc.*, 2008, **28**, 2099–2107.
17. Frommeyer, G. and Rosenkranz, R., In *Metallic Materials with High Structural Efficiency*, ed. Haddad. Kluwer Academic Publishers, Netherlands, 2004, pp. 287–308.
18. Tang, Z. H. and Williams, J. J., High temperature oxidation behavior of Ti_5Si_3-based intermetallics. *Intermetallics*, 2008, **16**, 1118–1124.
19. Vojtěch, D. and Novák, P., Surface protection of titanium by Ti_5Si_3 silicide layer prepared by combination of vapour phase siliconizing and heat treatment. *J. Alloy Compd.*, 2008, **464**, 179–184.
20. Schneibel, J. H. and Rawn, C. J., Thermal expansion anisotropy of ternary titanium silicides based on Ti_5Si_3. *Acta Mater.*, 2004, **52**, 3843–3848.
21. Rosenkranz, R., Frommeyer, G. and Smarsly, W., Microstructures and properties of high melting-point intermetallic Ti_5Si_3 and $TiSi_2$ compounds. *Mater. Sci. Eng. A*, 1992, **152**, 288–294.
22. Umakoshi, Y. and Nakashima, T., High-temperature deformation of Ti_5Si_3 single-crystals with $D8_{(8)}$ structure. *Scripta Metall. Mater.*, 1994, **30**, 1431–1436.
23. Williams, J. J. and Akinc, M., Oxidation resistance of Ti_5Si_3 and $Ti_5Si_3Z_x$ at 1000 °C (Z = C, N, or O). *Oxid. Met.*, 2002, **58**, 57–71.
24. Thom, A. J., Akinc, M., Cavin, O. B. and Hubbard, C. R., Thermal expansion anisotropy of Ti_5Si_3. *J. Mater. Sci. Lett.*, 1994, **13**, 1657–1660.
25. Williams, J. J., Ye, Y. Y., Kramer, M. J., Ho, K. M., Hong, L., Fu, C. L. *et al.*, Theoretical calculations and experimental measurements of the structure of Ti_5Si_3 with interstitial additions. *Intermetallics*, 2000, **8**, 937–943.
26. Thom, A. J., Young, V. G. and Akinc, M., Lattice trends in $Ti_5Si_3Z_x$ (Z = B, C, N, O and $0 < x < 1$). *J. Alloy Compd.*, 2000, **296**, 59–66.
27. Zhou, Y. C., Sun, Z. M., Chen, S. Q. and Zhang, Y., In-situ hot pressing/solid–liquid reaction synthesis of dense titanium silicon carbide bulk ceramics. *Mater. Res. Innovat.*, 1998, **2**, 142–146.
28. Sato, F., Li, J. F. and Watanabe, R., Reaction synthesis of Ti_3SiC_2 from mixture of elemental powders. *Mater. Trans.*, 2000, **41**(5), 605–608.
29. Izumi, F. and Ikeda, T., A Rietveld-analysis programme RIETAN-98 and its applications to zeolites. *Mater. Sci. Forum*, 2000, **321**, 198–203.
30. Zhou, Y. C., Zhang, H. B., Li, M. S., Wang, J. Y. and Bao, Y. W., Preparation of TiC free Ti_3SiC_2 with improved oxidation resistance by substitution of Si with Al. *Mater. Res. Innovat.*, 2004, **8**, 97–102.
31. Zhang, H. B., Zhou, Y. C., Bao, Y. W., Li, M. S. and Wang, J. Y., Intermediate phases in synthesis of Ti_3SiC_2 and $Ti_3Si(Al)C_2$ solid solutions from elemental powders. *J. Eur. Ceram. Soc.*, 2006, **26**, 2373–2380.
32. Leyland, A. and Matthews, A., On the significance of the H/E ratio in wear control: a nanocomposite coating approach to optimised tribological behaviour. *Wear*, 2000, **246**, 1–11.
33. Zum Gahr, K. H., Wear by hard particles. *Tribol. Int.*, 1998, **31**, 587–596.
34. He, Y. J., Winnubst, A. J. A., Schipper, D. J., Bakker, P. M. V., Burggraaf, A. J. and Verweij, H., Friction and wear behaviour of ceramic-hardened steel couples under reciprocating sliding motion. *Wear*, 1995, **184**, 33–43.
35. Sarkar, D., Manoj Kumar, B. V. and Basu, B., Understanding the fretting wear of Ti_3SiC_2. *J. Eur. Ceram. Soc.*, 2006, **26**, 2441–2452.
36. Huang, Z. Y., Zhai, H. X., Guan, M. L., Liu, X., Ai, M. X. and Zhou, Y., Oxide-film-dependent tribological behaviors of Ti_3SiC_2. *Wear*, 2007, **262**, 1079–1085.
37. Zhai, H. X., Huang, Z. Y., Zhou, Y., Zhang, Z. L., Wang, Y. F. and Ai, M. X., Oxidation layer in sliding friction surface of high-purity Ti_3SiC_2. *J. Mater. Sci.*, 2004, **39**, 6635–6637.
38. Basu, B., Vleugels, J., Kalin, M. and Van Der Biest, O., Friction and wear behavior of SiAlON ceramics under fretting contacts. *Mater. Sci. Eng. A*, 2003, **359**, 228–236.
39. Ouyang, J. H. and Sasaki, S., Tribo-oxidation of cathodic arc ion-plated (V, Ti)N coatings sliding against a steel ball under both unlubricated and boundary-lubricated conditions. *Surf. Coat. Technol.*, 2004, **187**, 343–357.
40. Fischer, T. E., Zhu, Z., Kim, H. and Shin, D. S., Genesis and role of wear debris in sliding wear of ceramics. *Wear*, 2000, **245**, 53–60.
41. Akhadejdamrong, T., Aizawa, T., Yoshitake, M., Mitsuo, A., Yamamoto, T. and Ikuhara, Y., Self-lubrication mechanism of chlorine implanted TiN coatings. *Wear*, 2003, **254**, 668–679.
42. Aizawa, T., Mitsuo, A., Yamamoto, S., Sumitomo, T. and Muraishi, S., Self-lubrication mechanism via the in situ formed lubricious oxide tribofilm. *Wear*, 2005, **259**, 708–718.